Tomographic pseudo-inversion of resistivity profiles

Pietro Cosentino and Dario Luzio
Istituto di Geofisica Mineraria, Università di Palermo, Italy

Abstract
A new approach to construct vertical and/or horizontal pseudosections starting from sets of resistivity (and/or IP) data is presented. In principle it consists in the division of the subsoil into a number of pixels (discretization), arranged in a 3D halfspace. The resistivity of each pixel is then obtained by a back-projection of the set of acquired experimental data, that is by arranging a set of convolutions using 3D filters. The coefficients of the filters are calculated, depending on the geometry of the electrode array used, on the basis of a mask reproducing the «influence coefficients» of all the pixels. The aim of these representations is to match the shape of the investigated structures as close as possible, so that, even if it can be considered a fast arrangement of the experimental data rather than a real inversion, it can be a useful tool in interpretation, at least as a simple preliminary sketch. This method is discussed, focussing on some critical choices regarding the construction of the filters and the use of smoothing factors; some applications on synthetic data calculated on simple models of buried resistive spheres are also presented.

Key words *pseudosection – pseudo-slices – resistivity profile – IP profile – pseudo-depth section – pseudo-inversion – back-projection – electric tomography*

1. Introduction

The concept of constructing a resistivity (or IP) pseudosection, *i.e.*, plotting the resistivity or IP data acquired along a profile in a vertical section, was first introduced by Hallof (1957), and in particular for the typical various-order dipole-dipole array. The first proposal was to plot all the apparent resistivity (or IP) data collected along the profile at the point of intersection of two 45 degree lines starting from the centers of the two (transmitter and receiver) dipoles right below the center of the whole dipole-dipole array (fig. 1).

Subsequently the practice of constructing such pseudosection was extensively applied by geophysicists all over the world. This is because the construction of the pseudosection is very easy and fast to carry out, whereas the inversion of the resistivity and IP data is in general a complex problem from the computing point of view, even for simple 2D models, especially when the available system has limited memory facilities.

Furthermore, the inversion of the experimental data, due to its non-linearity characteristics, has to be carried out using a starting model, so that a fast construction of the pseudosection is generally a very useful tool also as a preliminary step before the choice of the model for inversion.

Nevertheless, the use of the pseudosection has been subjected to different criticisms due to some negative characteristics: it neither gives an idea about the target depth nor means

Mailing address: Prof. Pietro Cosentino, Istituto di Geofisica Mineraria, Università di Palermo, Via M. Stabile 110, 90139 Palermo, Italy; e-mail: pietro.cosentino@unipa.it

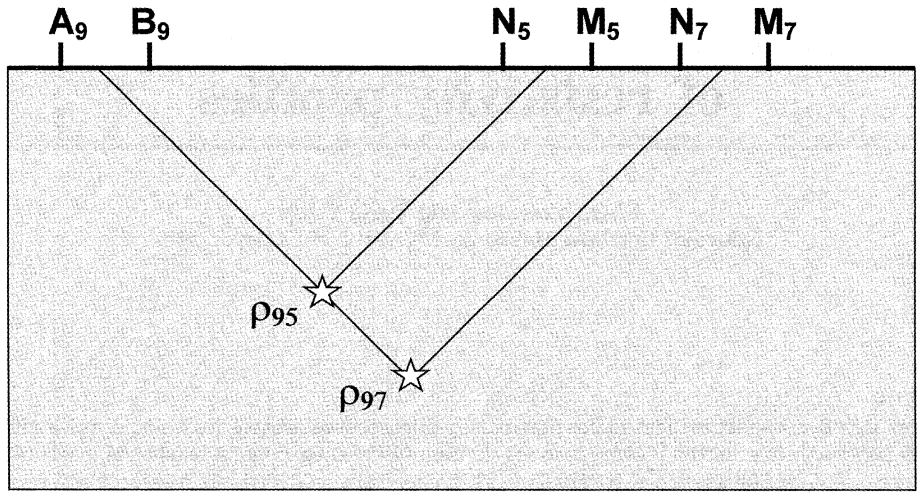

Fig. 1. Sketch of the construction of the dipole-dipole pseudosection proposed by Hallof (1957). The locations of two apparent resistivity values measured using the transmitter dipole No. 9 (A_9, B_9) and 5th and 7th order receiver dipoles are shown.

that the measured signal is coming from that depth (Apparao, 1991). These problems suggested many efforts and different attempts to improve the construction technique of the pseudosection and/or the way to extract information from it (for instance, to recognize the main lateral discontinuities in the pseudosections, see Fraser, 1981), especially the most desired one, regarding the real depth of the detected anomalies.

Edwars (1977) and Apparao (1991) have produced interesting approaches to change the scale of the pseudo-depths in the construction of pseudosections with the aim of improving the recognition of the real pseudo-depths of the detected anomalies. Later, Cosentino *et al.* (1995) and Moller *et al.* (1995) presented two slightly different approaches on 2D fast construction of pseudosections which can be considered significant innovations in the practice of 2D resistivity and/or IP interpretation. In fact, the former is in practice based on a convolution of experimental data

$$\rho(x, z) = \int g(x-\tau, z)\, \rho_a(\tau)\, d\tau \qquad (1.1)$$

using a $g(x-\tau, z)$ filter function which has been calculated on the basis of an approximated *influence factor* of each pseudosection pixel on the various resistivity data.

The second approach (Moller *et al.*, 1995) is based on a fast deconvolution of experimental data using the 2D Frechet kernel for the homogeneous halfspace and a subsequent inversion.

In this paper the approach already presented by Cosentino *et al.* (1995) and extended in Cosentino *et al.* (1997) is slightly improved and extended to a 3D modeling of the halfspace.

2. The influence factors

The previous paper (Cosentino *et al.*, 1995) calculated the influence factors of all the pixels of the selected mesh in the pseudosection on the basis of the anomaly of apparent resistivity due to an elementary resistive sphere centered on the pixel center.

Furthermore it has been observed (Cosentino *et al.*, 1997) that the weights calculated

in such a way are practically equivalent to those calculated in a discrete set of representative points of a homogeneous ground, by means of the formulas regarding the influence of the elementary volumes (Roy and Apparao, 1971) and four of the main configurations used for the construction of pseudosections (namely the linear symmetrical array of the α, β and γ tri-potential measurements (see Habberjam, 1979) and the n-th *order* dipole-dipole array) the influence factors have been calculated in a sufficiently large part of the overlying half-space.

The influence function of a point (x, y, z) of the subsoil on a resistivity measure carried out with a four-electrode linear array can be expressed as:

$$
\begin{aligned}
I(x, y, z) = {} & [(x - x_{C1})(x - x_{P1}) + y^2 + z^2] \cdot \\
& \cdot \{[(x - x_{C1})^2 + y^2 + z^2][(x - x_{P1})^2 + y^2 + z^2]\}^{-3/2} - \\
& - [(x - x_{C2})(x - x_{P1}) + y^2 + z^2] \cdot \\
& \cdot \{[(x - x_{C2})^2 + y^2 + z^2][(x - x_{P1})^2 + y^2 + z^2]\}^{-3/2} - \\
& - [(x - x_{C1})(x - x_{P2}) + y^2 + z^2] \cdot \\
& \cdot \{[(x - x_{C1})^2 + y^2 + z^2][(x - x_{P2})^2 + y^2 + z^2]\}^{-3/2} + \\
& + [(x - x_{C2})(x - x_{P2}) + y^2 + z^2] \cdot \\
& \cdot \{[(x - x_{C2})^2 + y^2 + z^2][(x - x_{P2})^2 + y^2 + z^2]\}^{-3/2}
\end{aligned}
\tag{2.1}
$$

where $(x_{C1}, 0, 0)$ and $(x_{C2}, 0, 0)$ are the coordinates of the current electrodes and $(x_{P1}, 0, 0)$ and $(x_{P2}, 0, 0)$ those of the potential electrodes.

The integrals of the contributions of the various elementary parts (pixels) are rather complex, especially because in some points of the subsoil relation (2.1) diverges and their elimination is rather critical. Therefore the problem has been solved by discretization, choosing a pixel mesh with a pixel size representing a compromise between the necessity to have small pixels and the opposite one to have a limited number of pixels in order to avoid too long a computer time in the subsequent back-projection. Therefore the necessary approximation is to consider homogeneous, inside the volume of pixels, the contribution to any apparent resistivity measure.

It is possible to define a partition level (hereafter *PL*) as the ratio between the smallest distance between two electrodes of the used array and the selected size of the pixel (which is considered unitary). The choice of *PL* ratio is important to define both the possible partition errors and the resolution power of the pseudo-section.

Some examples of the influence factors of the vertical «section» containing the pixels having an edge along the electrode line (since the pixel edges – not their centers – are centered in the origin of the selected reference system, the minimum offset is $y = 0.5$) are presented by means of contour lines. Figure 2a-d shows the influence factors referred to some equally spaced four-pole arrays useful for tripotential measurements (Habberjam, 1979), as well as the composed influence factors calculated for an array useful to evaluate the composed apparent resistivity ρ_μ (Cosentino and Luzio, 1994), which in general gives reliable estimates of the underground resistivity.

To show the behaviour of the influence coefficients *versus* the increasing of the dipole order, the influence factors for the 2nd, 3rd and 4th order dipole-dipole arrays are presented in fig. 3; whereas to introduce a 3D reconstruction, the influence factors of different sections parallel to a Wenner resistivity measurement (offset distance y increasing from 0.5 to 4.5, of course with respect to the size of the pixel edge) are shown in fig. 4. It can be observed that, even though the general trends of the factors (also the weight values in the lower part) are very similar – due to the use of the same array – in the upper part the weights – both positive and negative – become smaller and smaller according to their increasing distances from the electrodes.

It is obvious that the influence factor of a pixel decreases with its distance from the electrodes: the number of the pixels in which the value of the influence factor remains signifi-

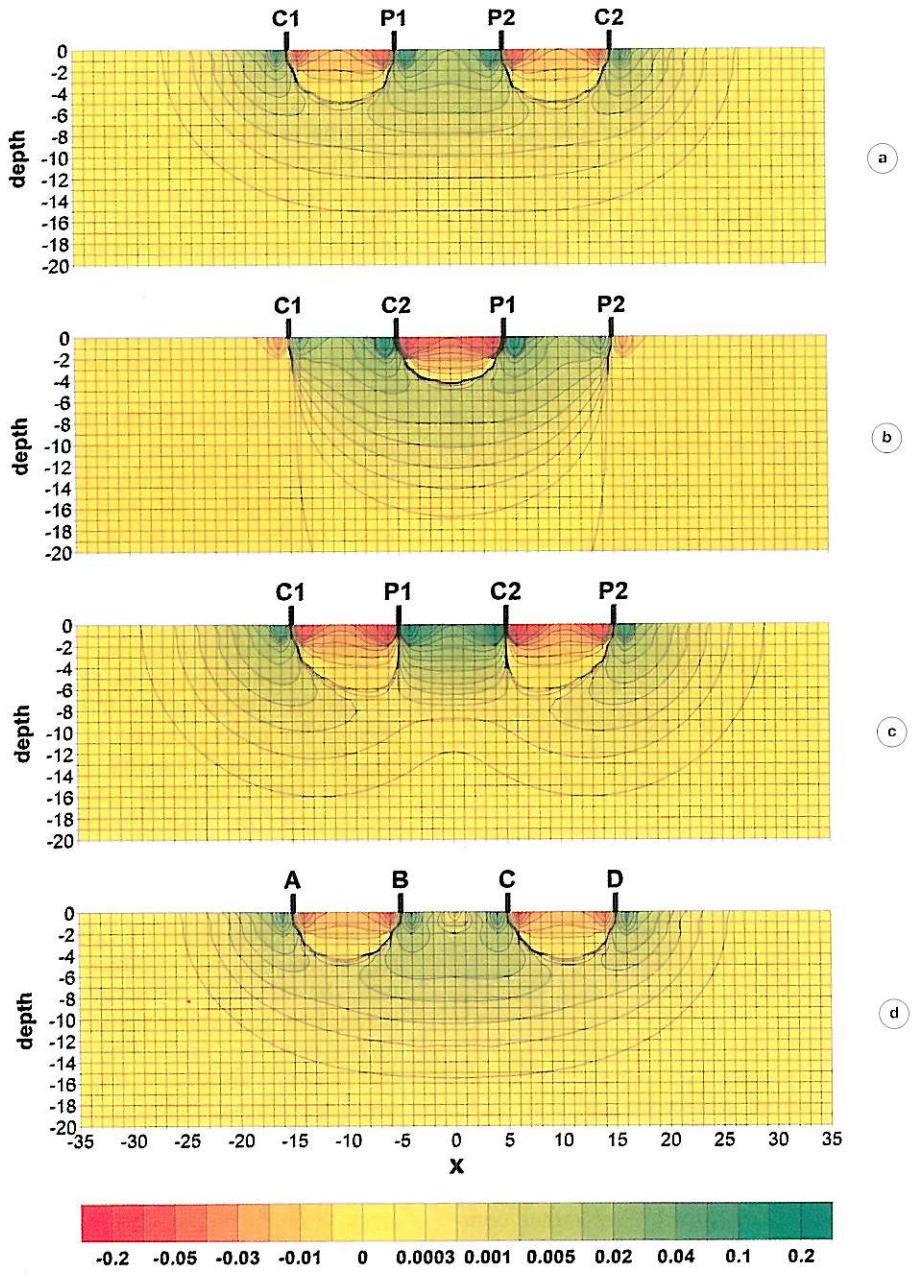

Fig. 2a-d. Influence factors for a single apparent-resistivity measure carried out using Wenner array α-tripotential (a), β-tripotential (b) and γ-tripotential (c). The influence coefficients represented in the bottom of the figure (d) refer to a tripotential array useful to calculate the values of ρ_μ: in this case the electrodes A, B, C and D can be used both for current and potential, depending on the combination used. In all cases the offset $y = 0.5$ and partition level $(PL) = 10$.

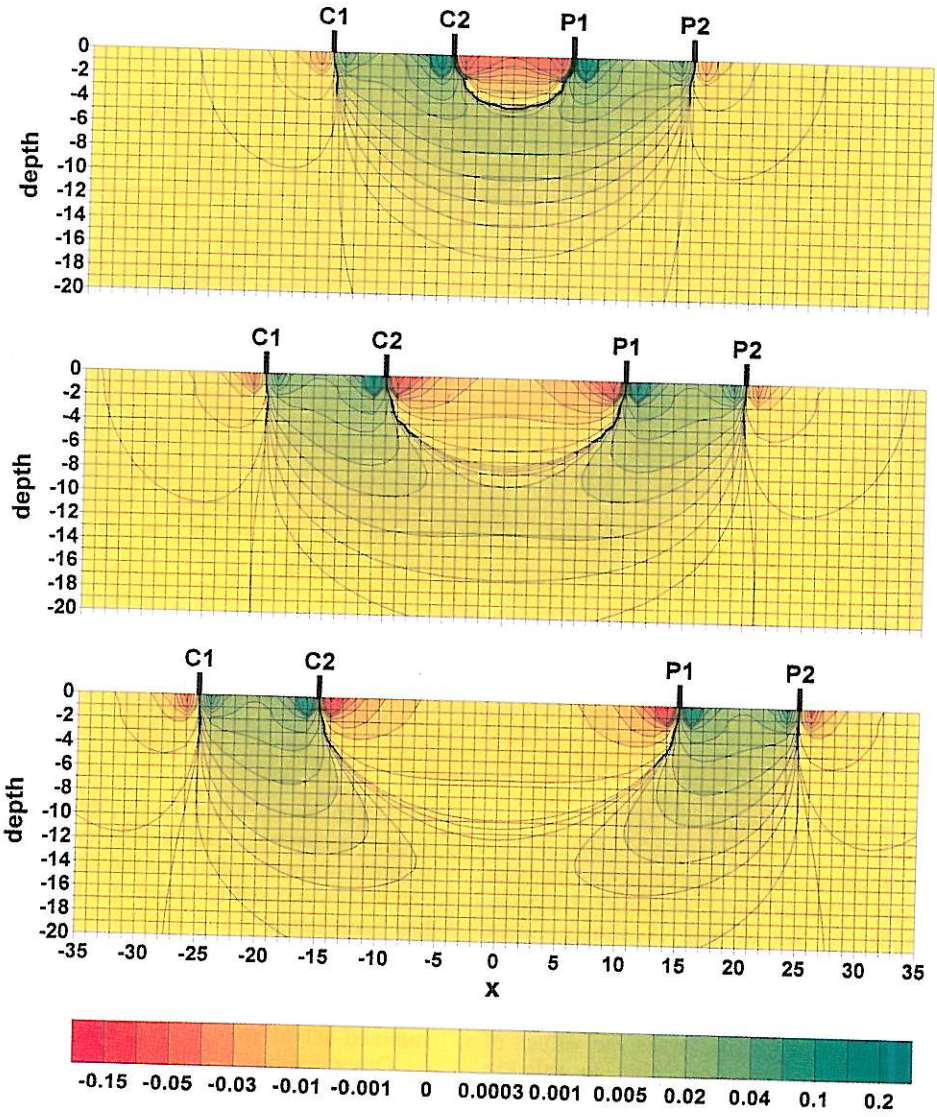

Fig. 3. Influence factors for a single apparent-resistivity measure carried out using 2nd (top), 3rd (center) and 4th (bottom) order dipole-dipole array, offset $y = 0.5$ and partition level (PL) = 10.

cant depends on the PL ratio, the dimensions of the «investigated volume» basically depending on the dimensions of the array.

It is important to note that the influence factors for an apparent resistivity measurement are positive in a (generally large) part of the influence volume and are negative in (generally restricted) parts of the subsoil, mostly located very close to the electrodes. If the influence coefficient of a pixel is positive, it means that an increment of resistivity in the pixel will produce an increment of the measured apparent resistivity: the negative coefficients will work in the opposite way.

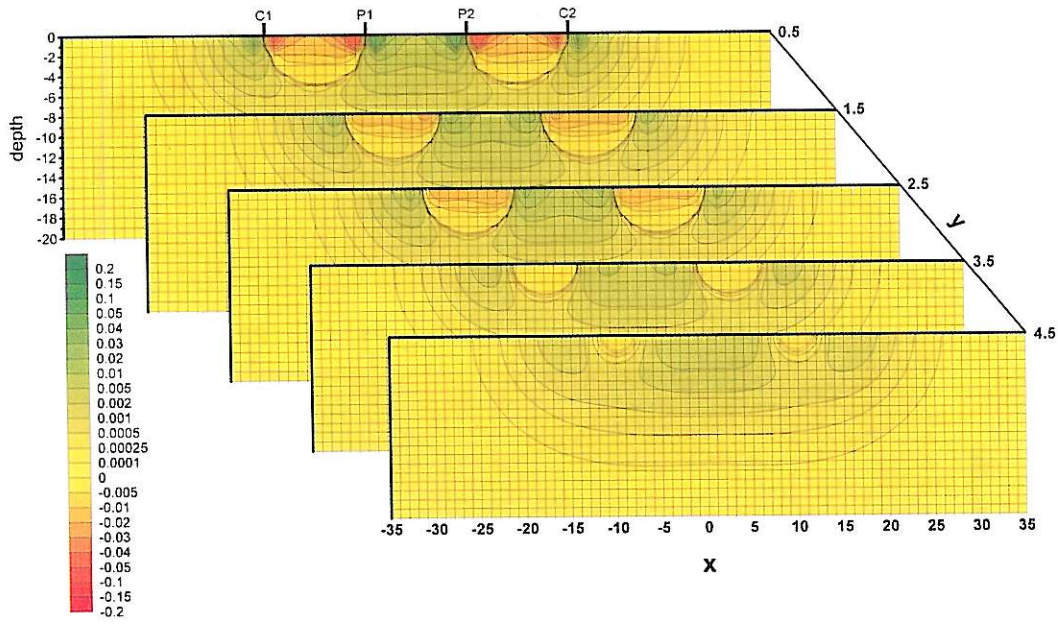

Fig. 4. Influence factors of five sections of pixels parallel to a single apparent-resistivity measure carried out using a Wenner array (α-tripotential), offset $y = 2.5$ and partition level (PL) = 10.

3. Data pseudo-inversion

The influence factors represent the basis to start a back-projection to reconstruct the resistivity model of the subsoil. A simple linear procedure can be used which, starting from the apparent resistivity values measured along several profiles and using suitable filters obtained from the influence factors, gives the values of every pixel resistivity, according to relation (1.1).

The computation of the various filter coefficients is critical: in fact the necessity of a normalization of the coefficients becomes rather difficult because of the presence of negative values in the various sets of influence factors.

Two different methods have been tested to overcome this problem. In principle one can conceive that for the back-projection all the coefficients should be taken in their absolute value, which indicates the degree of influence, whereas the possible negative sign can be assumed to be included in the decreased corresponding experimental resistivity value. Therefore the absolute values of the influence factors can be normalized to produce a filter set which has been tested using synthetic data.

Another possibility is to set to zero the negative coefficients, so that only the positive influence factors should be used to build a normalized set of filter coefficients.

Other methods of processing the influence factors to obtain the filter coefficients can be adopted: in this respect some tests have been performed without significant results, other tests will be carried out in the future.

A simple model has been used to calculate the synthetic data to be used for the back-projections. The model consists in a buried resistive sphere, with infinite resistivity embedded in a homogeneous ground with resistivity equal to 1 Ω m (fig. 5).

Various sets of synthetic data referring to the same array but different PL values as well as different parallel profiles have been used to

execute the back-projections. Figures 6, 7, 8, 9, 10 and 11 show some examples of back-projections: the size and position of the sphere are marked in white, whereas both the above methods of calculating the filters have been tested.

Figure 12 shows a pseudosection carried out using a single profile of resistivity data and a single array moved along the profile. The construction of a pseudosection using the classical (or slightly modified) methods (Hallof, 1957, see fig. 1) cannot be accomplished because all the data acquired using an array with fixed electrode distances have to be referred to a single depth of the pseudosection.

Figure 12 (bottom) represents a pseudosection built with part of the data used to assemble the lowest pseudosection of fig. 11: in fact this last contains also data coming from the same profile (acquired with different *PL* values) as well as data acquired along ten other profiles characterized by offset values ranging from $y = -9.5$ to $y = 10.5$ with step = 1. The comparison between figs. 11 (bottom) and 12 (bottom) shows that the overlapping of many (and different) data acquired in the same area along parallel profiles. Even though it is of course a very important constraint to define the buried structures and to increase the reliability of the reconstruction, it does not increase the intensity of the resistivity anomaly. Probably, the assembly of different profiles can be still improved and optimized.

Finally, some horizontal pseudo-slices referring to the large sphere model are presented, respectively for ρ_β (fig. 13) and ρ_μ (fig. 14), using both the tested filters. For comparison, fig. 15 represent two sets of pseudo-slices carried out using the classical way (fig. 1) to construct 3D pseudosections and pseudo-slices.

4. Conclusions and possible improvement of the technique

The pseudosections and the horizontal pseudo-slices obtained using back-projection the technique here proposed seem to have much more resolving power than those obtained in the classical way, even if the resistivity contrasts are generally lower. Therefore, since a significant noise can strongly influence the resulting maps, it is essential to use reliable and «clean» experimental data: the tripotential method (Habberjam, 1979), for instance, seems to be a very useful tool for this purpose.

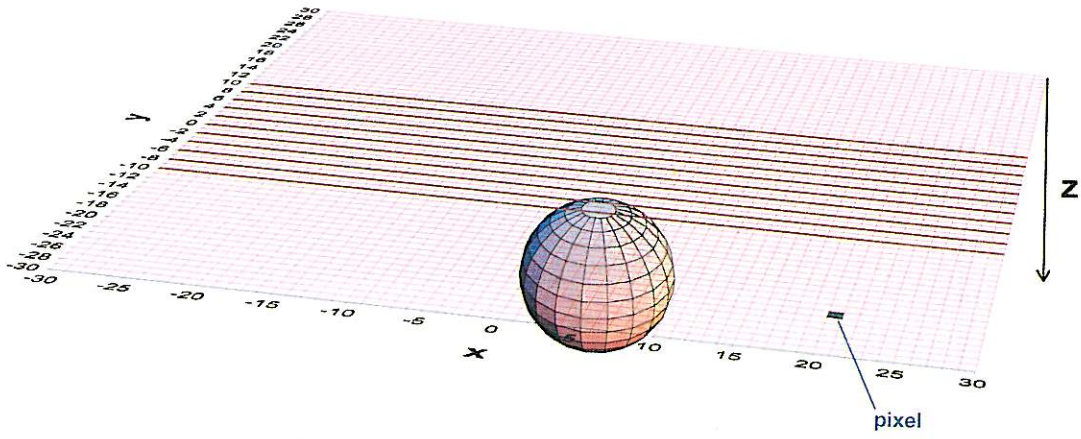

Fig. 5. Perspective representation of the models for which the synthetic data have been calculated along profiles (dark lines) and the back-projections have been carried out. Two models of a buried resistive sphere have been tested, both centered in the point $x = 0$, $y = 0$, the former having center at $z = 6$ and radius = 4 (large sphere), the latter $z = 4$ and radius = 2 (small sphere).

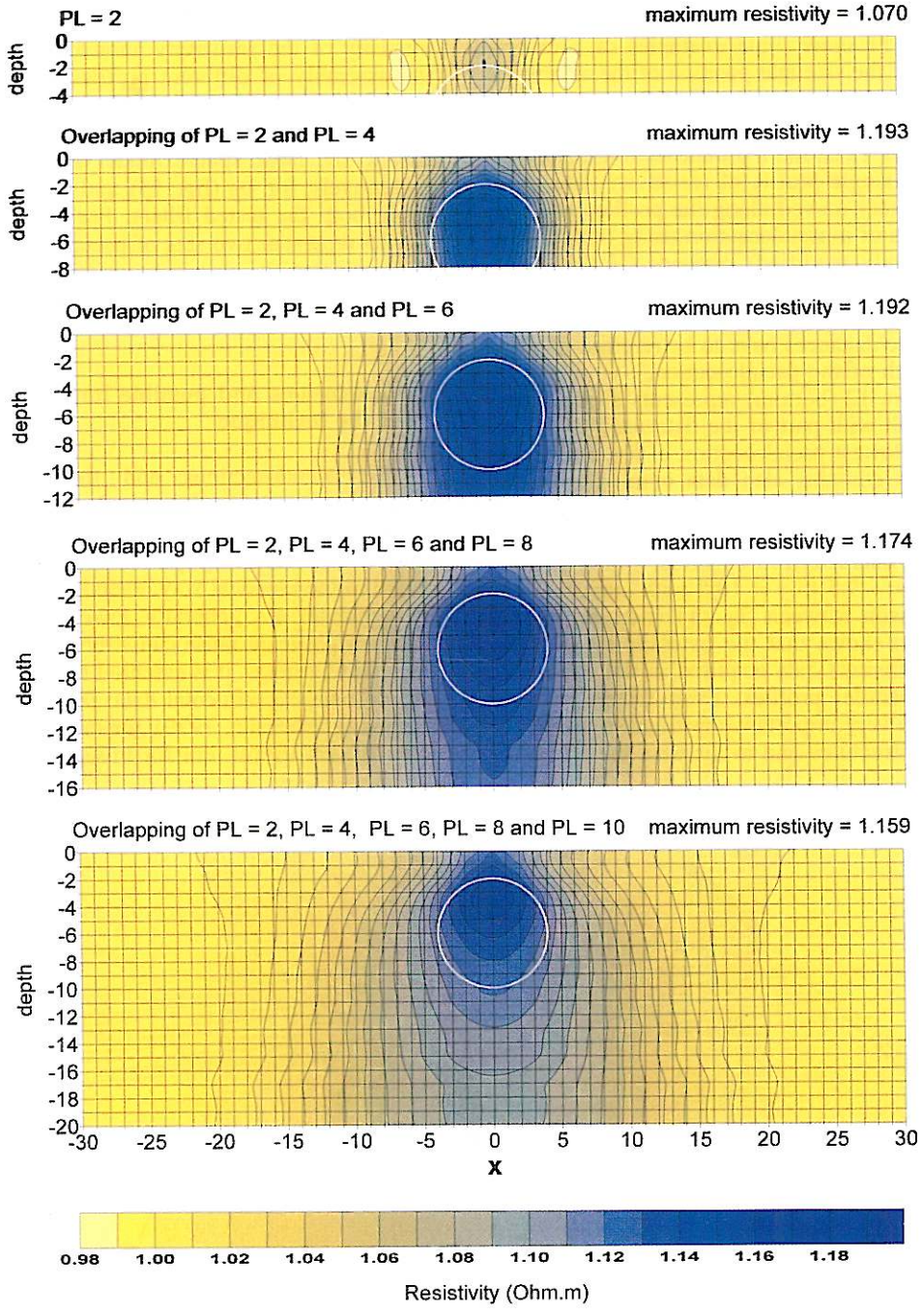

Fig. 6. The large sphere model. 3D pseudosections of the tripotential composed resistivity ρ_μ obtained using filters derived from only positive influence factors.

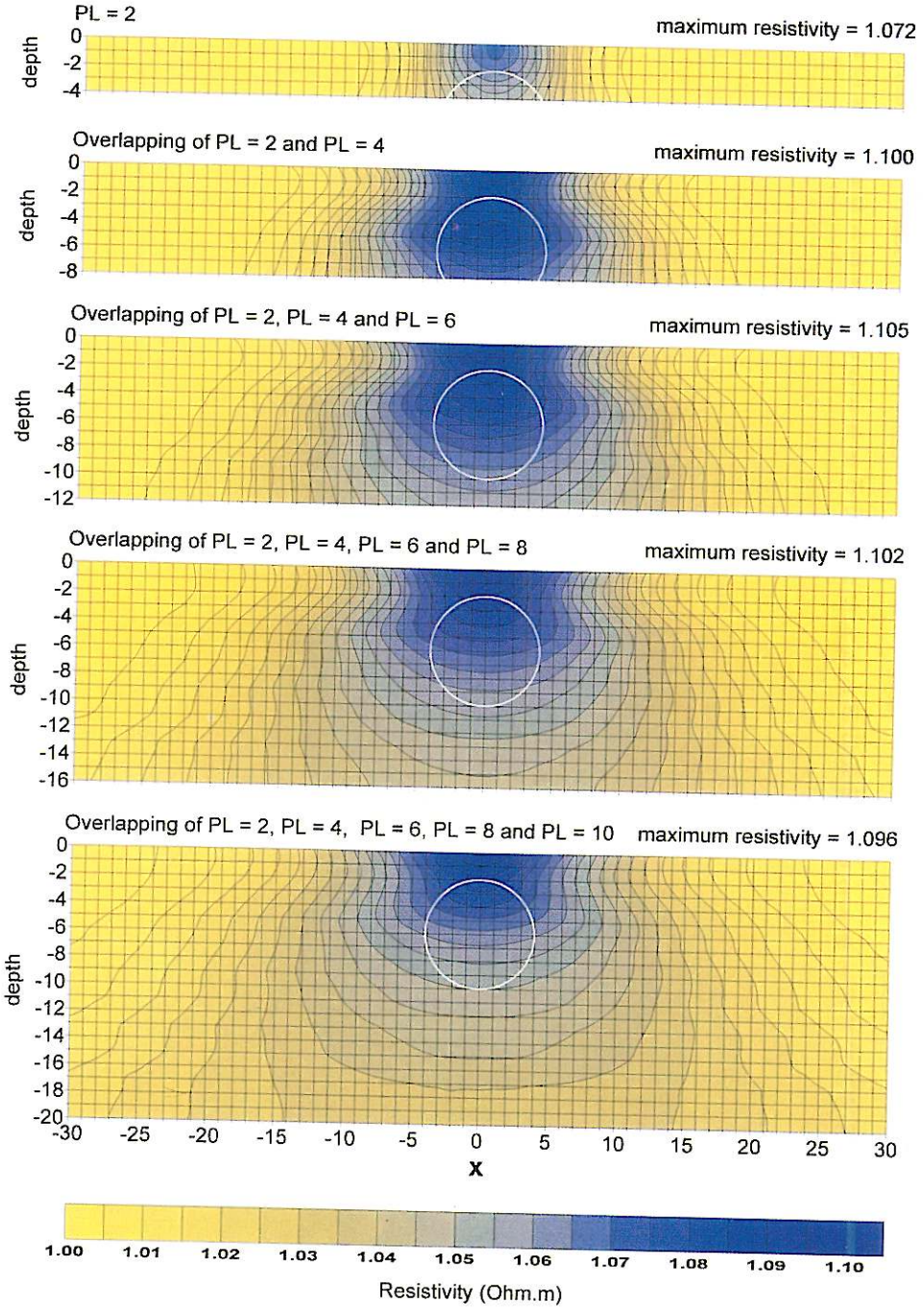

Fig. 7. The large sphere model. 3D pseudosections of the tripotential composed resistivity ρ_μ obtained using filters derived from absolute values of the influence factors.

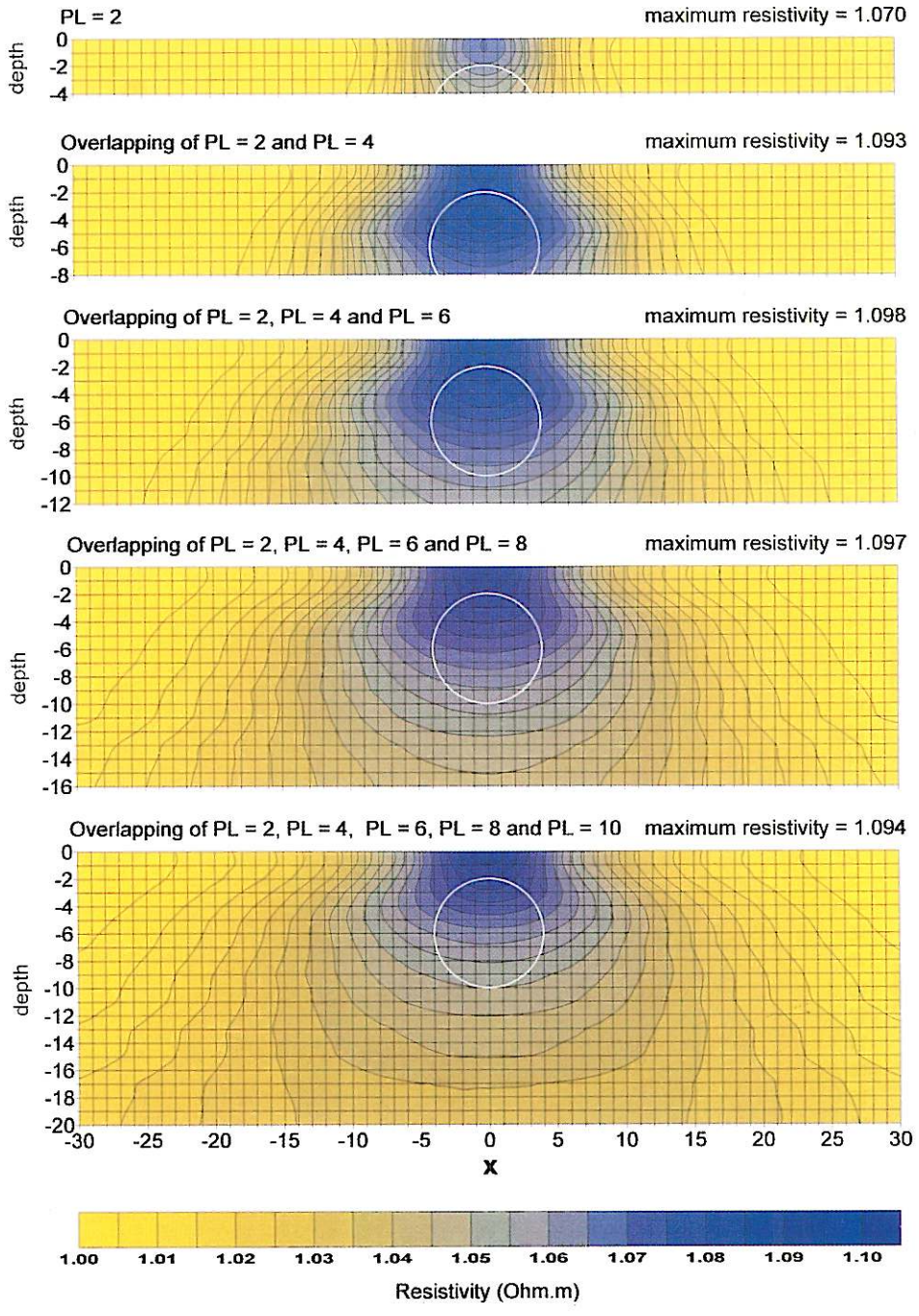

Fig. 8. The large sphere model. 3D pseudosections of the tripotential composed resistivity ρ_β obtained using filters derived from only positive influence factors.

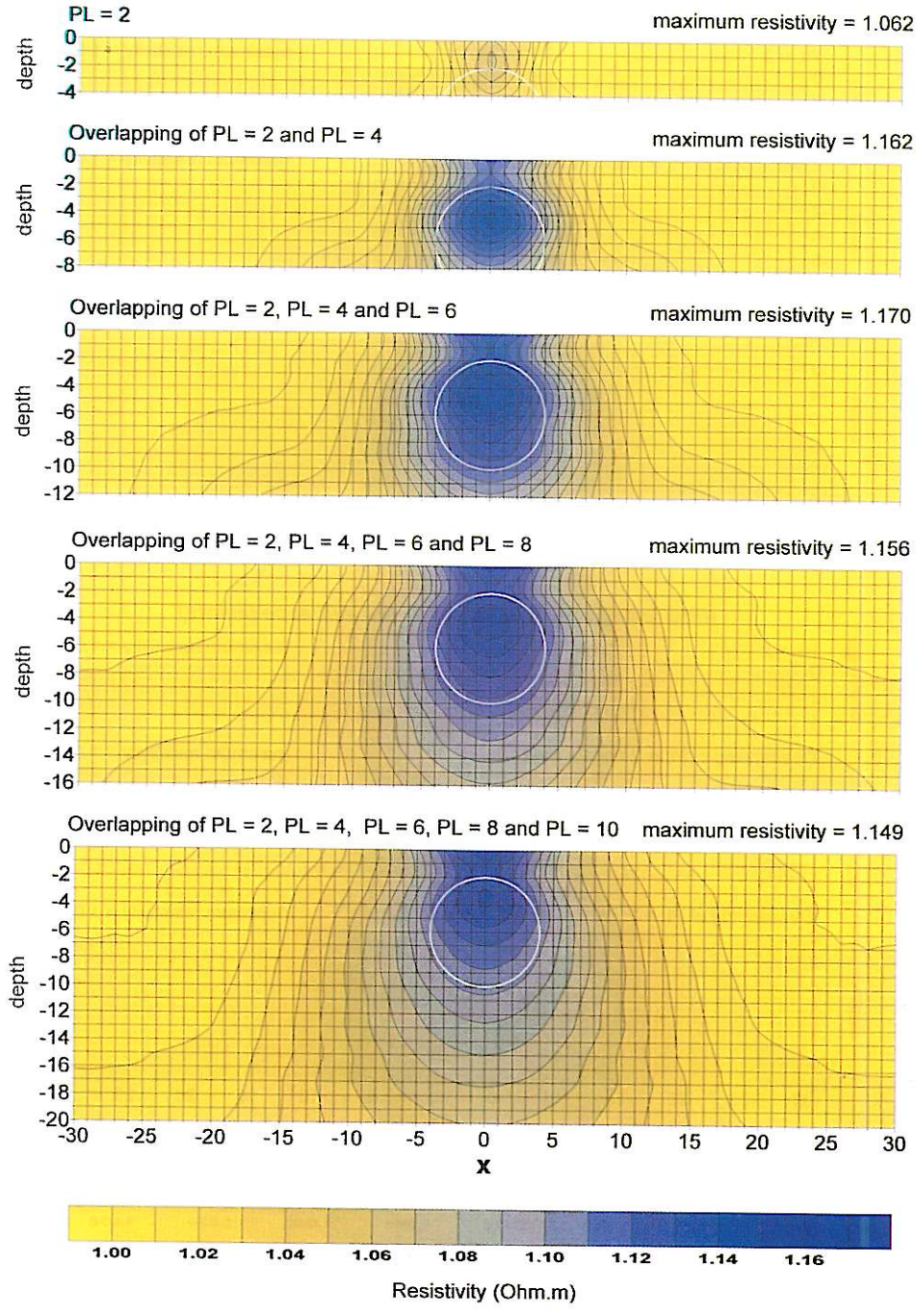

Fig. 9. The large sphere model. 3D pseudosections of the tripotential composed resistivity ρ_β obtained using filters derived from absolute values of the influence factors.

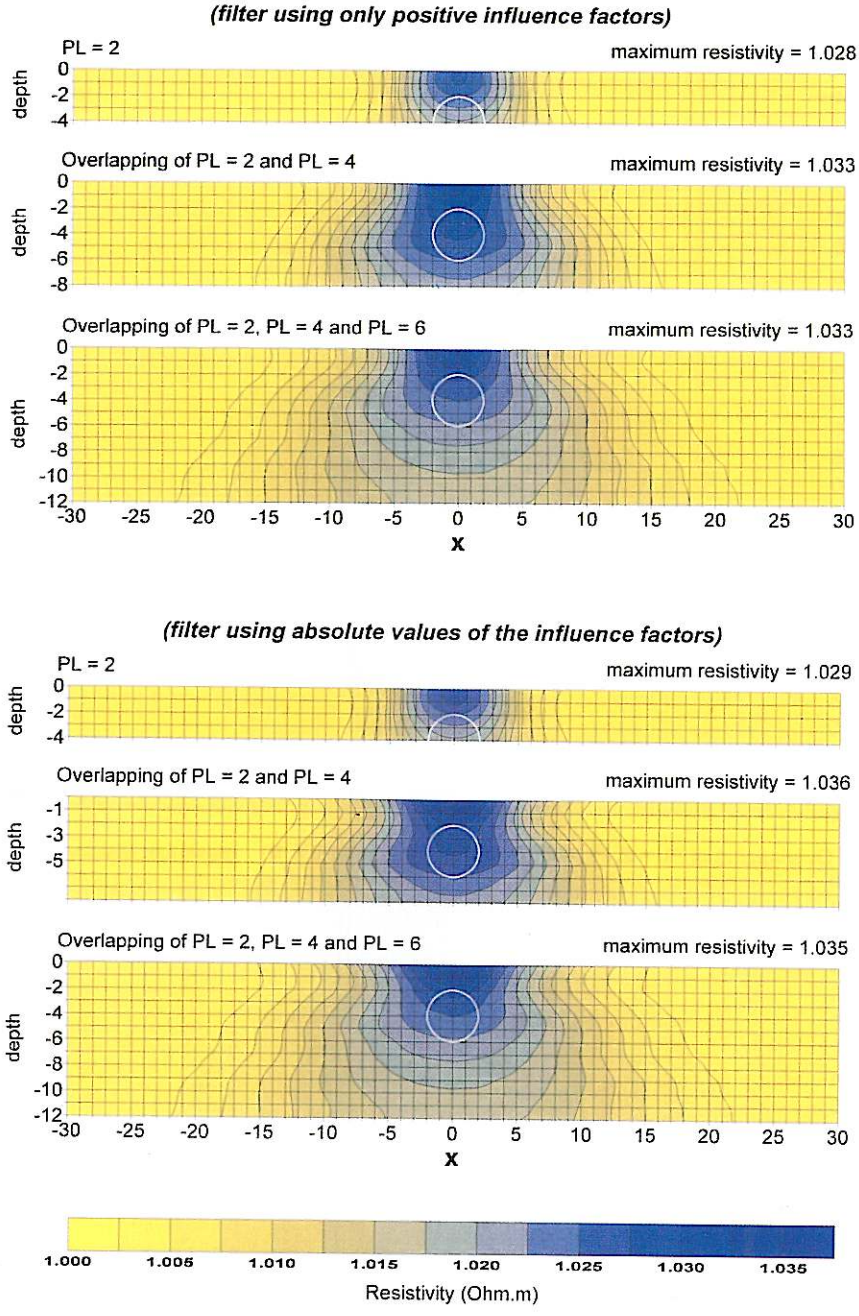

Fig. 10. The large sphere model. 3D pseudosections of the tripotential composed resistivity ρ_μ obtained using filters derived from only positive influence factors (top) and those derived from absolute values of the influence factors (bottom).

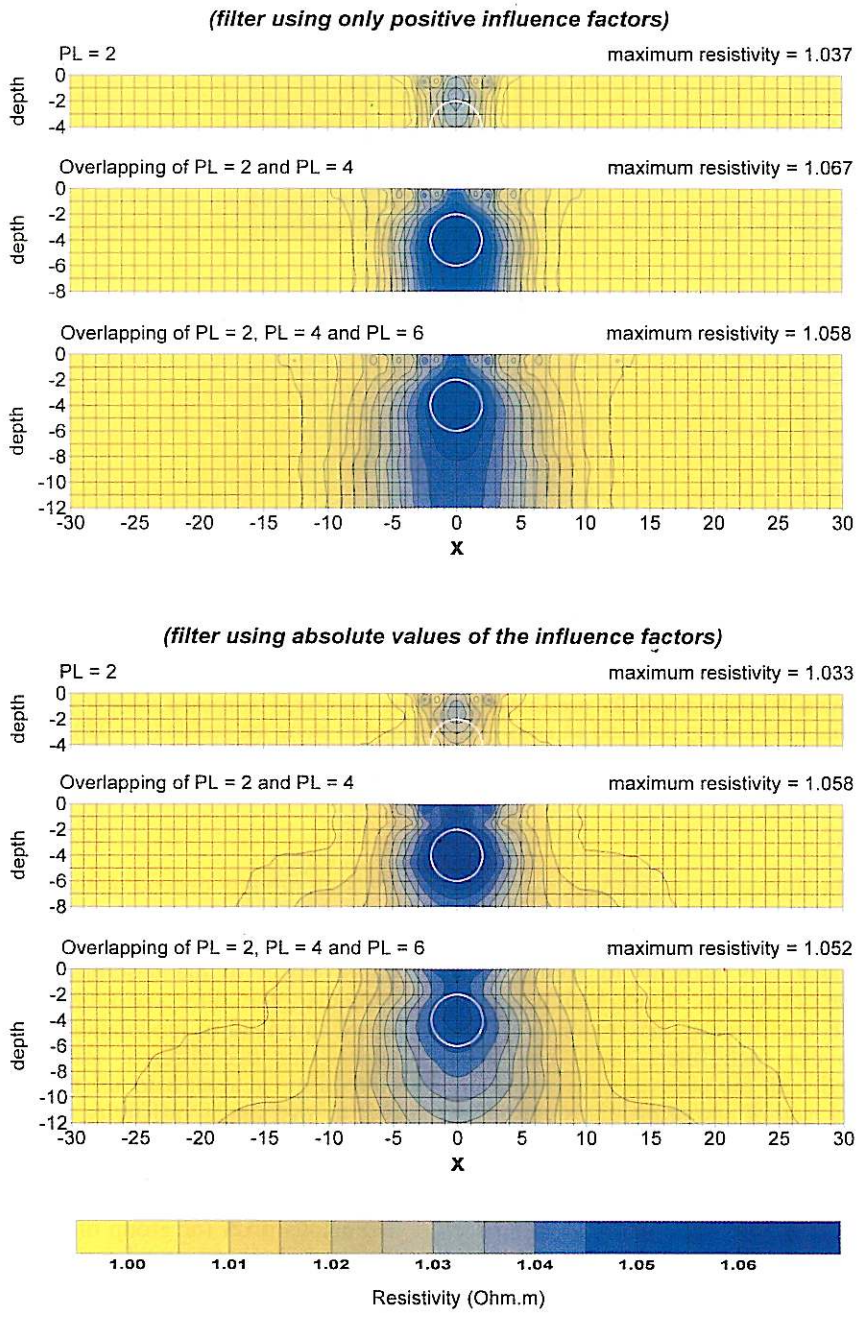

Fig. 11. The large sphere model. 3D pseudosections of the tripotential composed resistivity ρ_β obtained using filters derived from only positive influence factors (top) and those derived from absolute values of the influence factors (bottom).

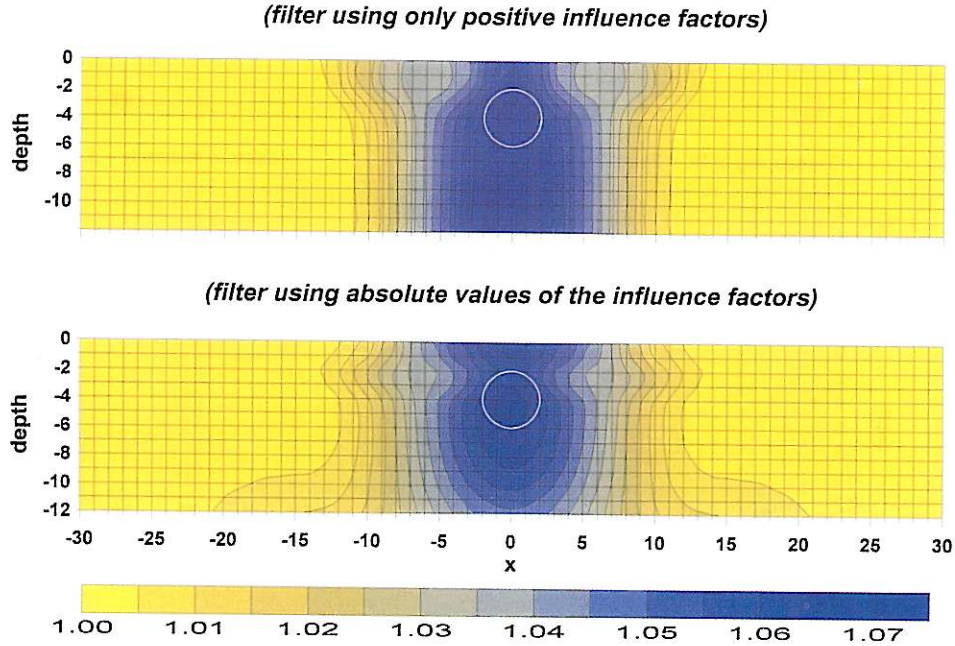

Fig. 12. The small sphere model. 2D pseudosections of the tripotential composed resistivity ρ_β obtained using a single profile of resistivity data and an array ($PL = 6$) moved along the profile ($y = 0.5$). A filter was used derived from only positive influence factors (top) and one derived from absolute values of the influence factors (bottom).

The main difficulties to convert the influence factors into the filter coefficients derive from the presence of negative and positive factors. It is also very difficult to arrange into suitable non-normalized filters both negative and positive coefficients: the reason why the attempts to use such filters failed may also be connected with the necessary discretization of both the set of experimental field measurements and the model of the pseudo-inversion.

The two tested methods to select the filter coefficients (absolute values of the influence factors or only positive values) gave generally minor differences in the results; the use of absolute values of the influence factors generally outlines the shapes of the resistivity models better than the use of positive values, especially in their lower parts. Significant differences in the shape of the reconstructed pseudosections strongly depend on the different arrays used.

However, it is possible to introduce some improvement to the described techniques. In particular, the filter coefficients can be subjected to a kind of modulation which accounts mainly for the different level of combined probability to assign to all the pixels giving rise to the single resistivity anomalous measurements. The distribution of that value to all the pixels which can influence it does not take into account the effective origin, *i.e.*, the real anomalous pixel (or group of pixels) to which the anomalous measured resistivity should be entirely ascribed.

Furthermore, the back-projection of the experimental data does not distinguish a near pixel from an equivalent number of farther pixels, so that some new constraints can be introduced to account for this problem.

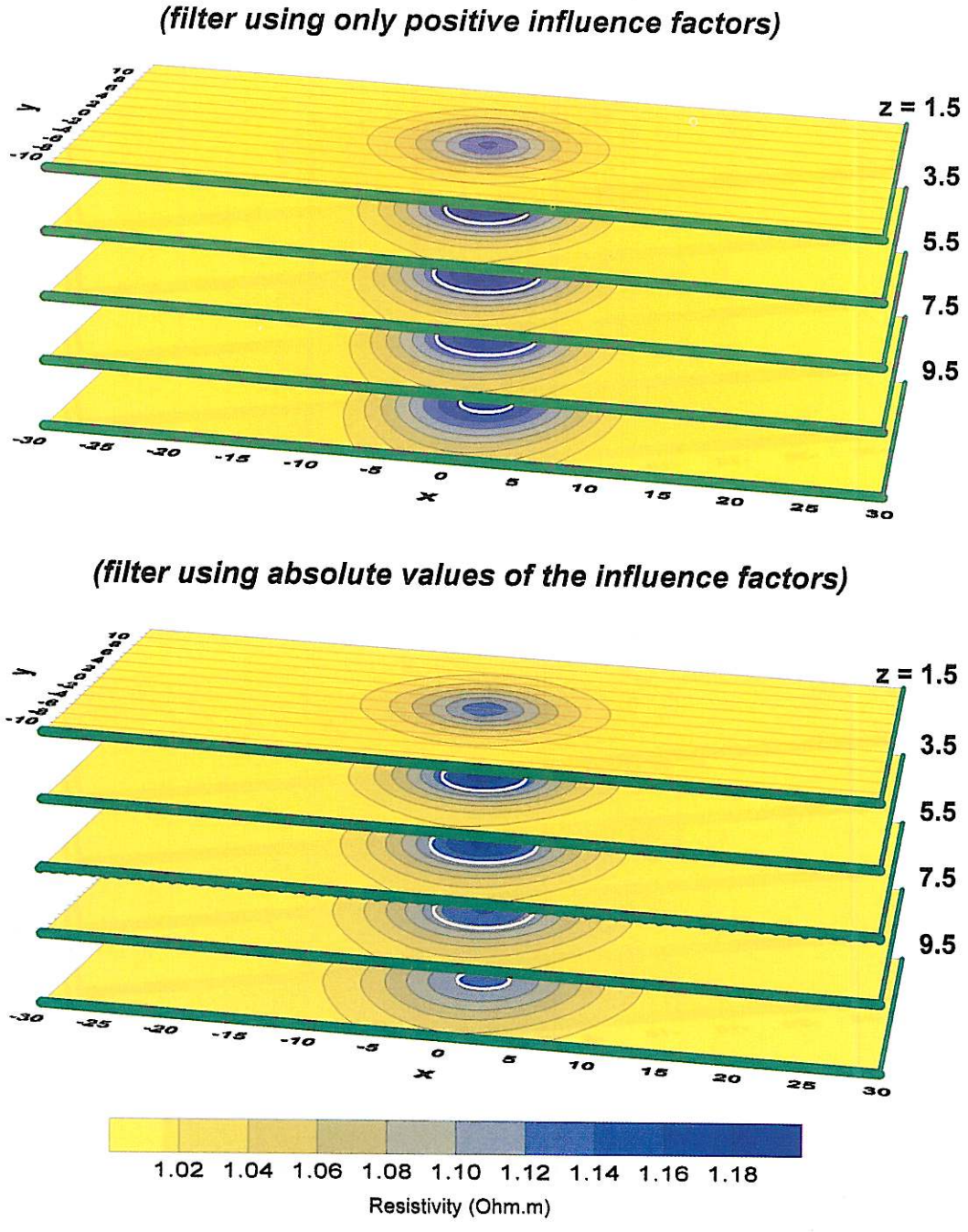

Fig. 13. The large sphere model. 3D horizontal pseudo-slices of the ρ_β resistivity, obtained using the two filtering coefficient sets.

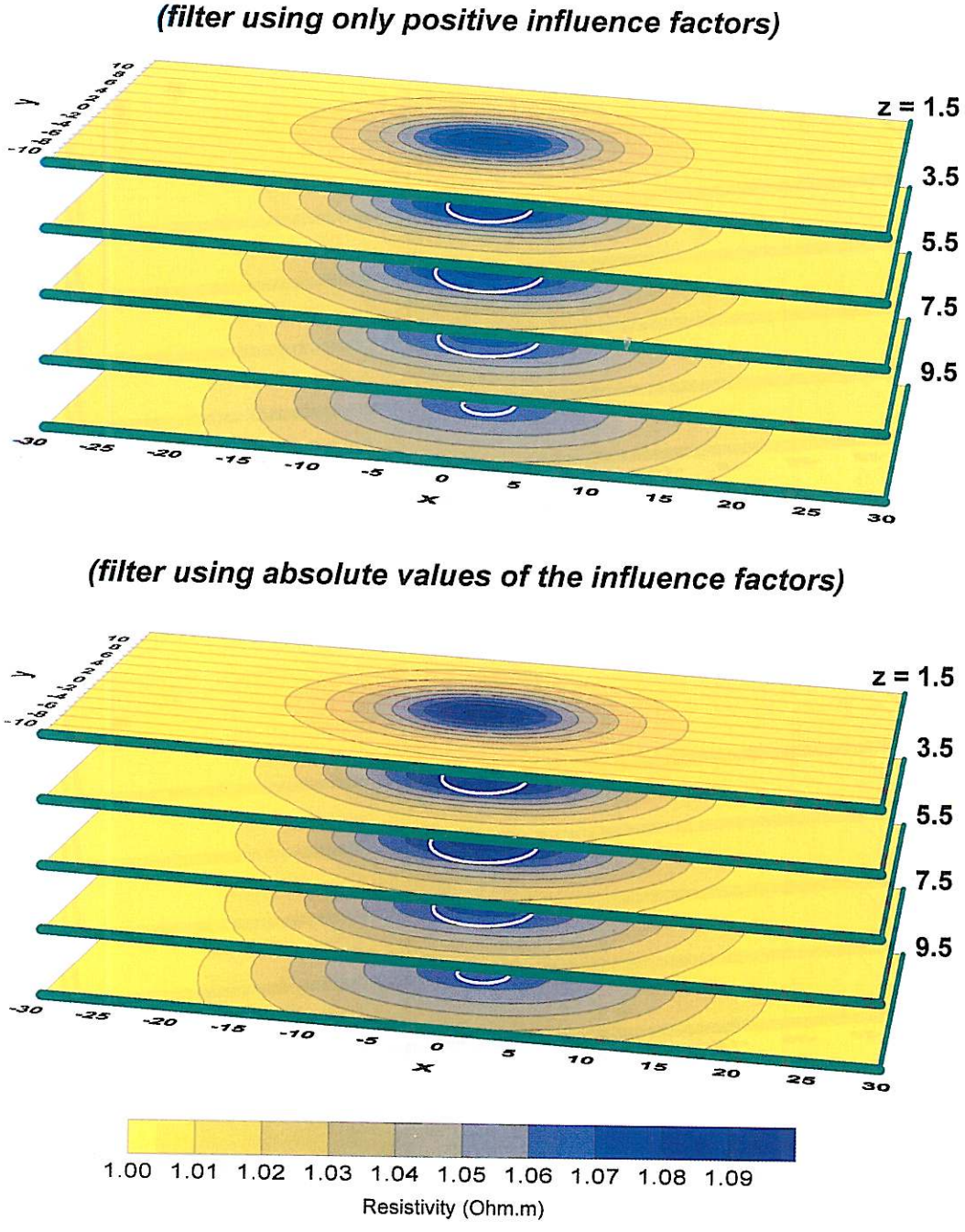

Fig. 14. The large sphere model. 3D horizontal pseudo-slices of the ρ_u composed resistivity, obtained using the two filtering coefficient sets.

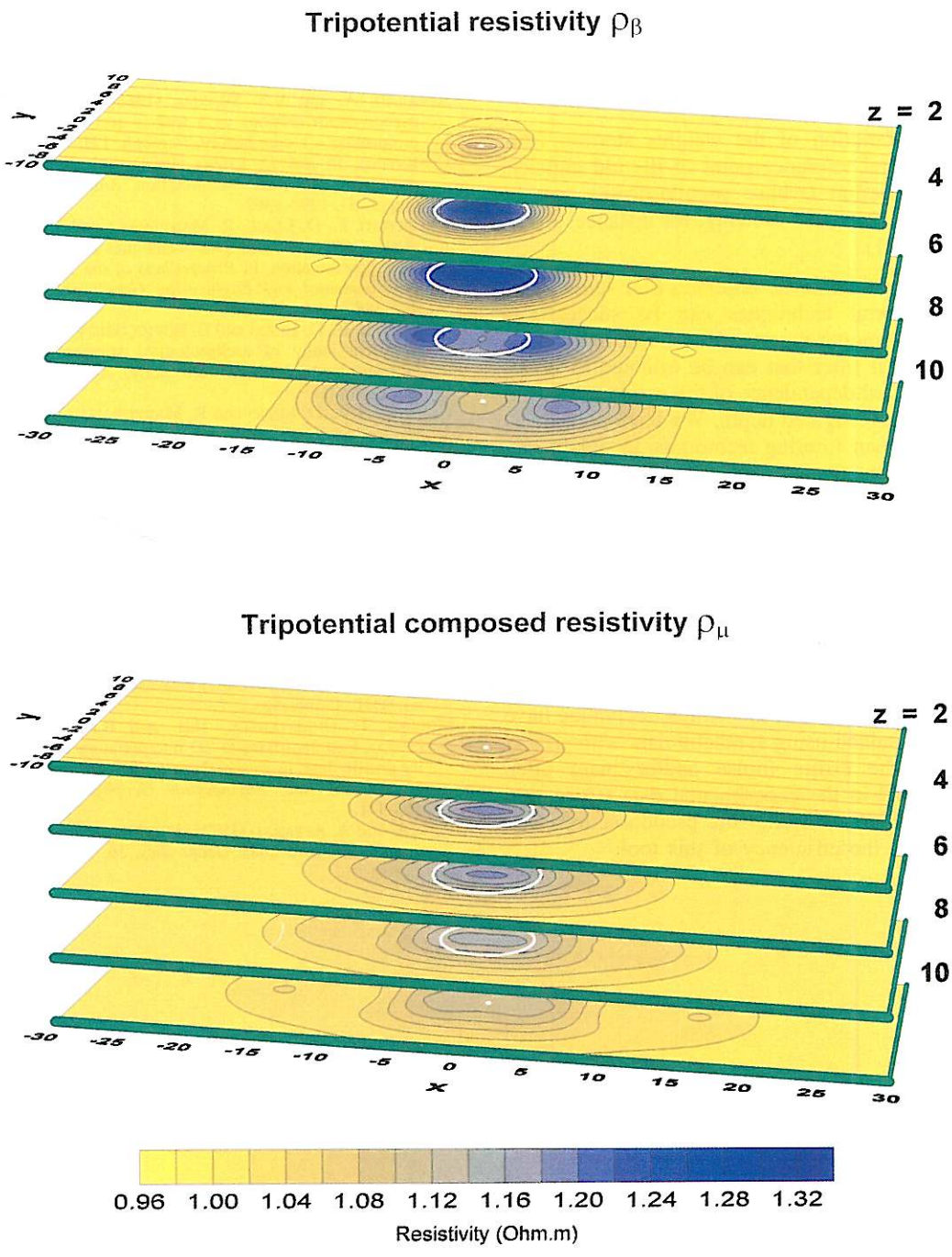

Fig. 15. 3D horizontal pseudo-slices of the ρ_β resistivity (top) and ρ_μ composed resistivity (bottom), obtained for the model of the large buried resistive sphere using the classical pseudosection construction shown in fig. 1.

Therefore some modulations of coefficients can involve:

1) Variations of the weights with the distance from the used array.

2) Variation of the weights starting from the central reference point of the old classical pseudosection (whose pseudo-depths can be slightly changed following, for instance, Apparao, 1991).

It should also be observed that some filtering general techniques can be successfully used to smooth the pseudosections, including a horizontal filter that can be oriented to reproduce a real dependence of the resolution power on the investigated depth. We have used many well-chosen filtering techniques to obtain representations (pseudosections and pseudo-slices) as alike as possible to the synthetic models, and interesting results have been obtained. Since these results are probably influenced by our knowledge about the characteristics of the synthetic models, we are now trying to find more general filtering processes.

Finally the conclusions have to include a marker point to avoid possible disillusion: the promising results of this simple technique have been obtained using synthetic data without any noise, the errors (noise and/or bias) often contained in the experimental data (Cosentino *et al.*, 1996) can alter the pseudosections and decrease the efficiency of this tool.

REFERENCES

APPARAO, A. (1991): Geoelectric profiling, *Geoexploration*, **27**, 351-389.

APPARAO, A. and V.S. SHARMA (1983): The modified pseudo-depth sections as a tool in resistivity and IP prospecting – a case history, *Pageoph*, **121**, 91-108.

COSENTINO, P. and D. LUZIO (1994): Tripotential data processing for HES interpretation, *Ann. Geofis.*, **37** (suppl. 5), 1295-1302.

COSENTINO, P., D. LUZIO, R. MARTORANA and L. TERRANOVA (1995): Tomographic techniques for pseudosection representation, in *Proceedings of the 1st Meeting Environmental and Engineering Geophysics*, Torino, 485-488.

COSENTINO, P., D. LUZIO and E. ROTIGLIANO (1996): Geoelectrical study of archaeological structures in the Himera plane (North-Western Sicily), *Ann. Geofis.*, **39** (1), 109-121.

COSENTINO, P., D. LUZIO and R. MARTORANA (1997): Filters for fast 2D and 3D pseudo-inversion of the resistivity profiles, in *Proceedings of the 1st Meeting Environmental and Engineering Geophysics, Aarhus*, 367-370.

EDWARDS, L.S. (1977): A modified pseudosection for resistivity and IP, *Geophysics*, **42**, 1020-1036.

FRASER, D.C. (1981): Contour map presentation of dipole-dipole induced polarization, *Geophys. Prospect.*, **29**, 639-651.

HABBERJAM, G.M. (1979): Apparent resistivity observations and the use of square array techniques, *Gerbruder Borntraeger*, Berlin, 152.

HALLOF, P.G. (1957): On the interpretation of the resistivity and induced polarization measurements, *Ph.D. Thesis*, MIT, Cambridge.

MOLLER, I., CHRISTENSEN, N.B. and B.H. JACOBSEN (1995): Fast approximate 2D interpretation of resistivity profile data, in *Proceedings of the 1st Meeting Environmental and Engineering Geophysics*, Torino, 468-471.

ROY, A. and A. APPARAO (1971): Depth of investigation in direct current methods, *Geophysics*, **36**, 943-959.